Surface structures of In-Pd intermetallic compounds. I. Experimental study of In thin films on Pd(111) and alloy formation

Garry Mcguirk, Julian Ledieu, Émilie Gaudry, Marie-Cécile de Weerd, Vincent Fournée

▶ **To cite this version:**

Garry Mcguirk, Julian Ledieu, Émilie Gaudry, Marie-Cécile de Weerd, Vincent Fournée. Surface structures of In-Pd intermetallic compounds. I. Experimental study of In thin films on Pd(111) and alloy formation. Journal of Chemical Physics, 2014, 141 (8), pp.084702. 10.1063/1.4892408 . hal-01075808

HAL Id: hal-01075808
https://inria.hal.science/hal-01075808

Submitted on 20 Oct 2014

HAL is a multi-disciplinary open access archive for the deposit and dissemination of scientific research documents, whether they are published or not. The documents may come from teaching and research institutions in France or abroad, or from public or private research centers.

L'archive ouverte pluridisciplinaire **HAL**, est destinée au dépôt et à la diffusion de documents scientifiques de niveau recherche, publiés ou non, émanant des établissements d'enseignement et de recherche français ou étrangers, des laboratoires publics ou privés.

Surface structures of In-Pd intermetallic compounds. I. Experimental study of In thin films on Pd(111) and alloy formation

G. M. McGuirk, J. Ledieu, É. Gaudry, M.-C. de Weerd, and V. Fournée
Institut Jean Lamour (UMR7198 CNRS-Nancy-Université de Lorraine), Parc de Saurupt, 54011 Nancy Cedex, France

(Received 29 April 2014; accepted 5 June 2014; published online 25 August 2014)

A combination of experimental methods was used to study the structure of In thin films deposited on the Pd(111) surface and the alloying behavior. X-ray photoelectron spectroscopy (XPS), low-energy electron diffraction (LEED), and scanning tunneling microscopy results indicate that surface alloying takes place at room temperature. Below 2 monolayer equivalents (MLEs), the LEED patterns show the formation of three rotational domains of InPd(110) of poor structural quality on top of the Pd(111) substrate. Both core-levels and valence band XPS spectra show that the surface alloy does not yet exhibit the electronic structure characteristic of the 1:1 intermetallic compound under these conditions. Annealing the 1 MLE thin film up to 690 K yields to a transition from a multilayer InPd near-surface intermetallic phase to a monolayer-like surface alloy exhibiting a well ordered ($\sqrt{3} \times \sqrt{3}$) R30° superstructure and an estimated composition close to In_2Pd_3. Annealing above 690 K leads to further In depletion and a (1 × 1) pattern is recovered. The ($\sqrt{3} \times \sqrt{3}$) R30° superstructure is not observed for thicker films. Successive annealing of the 2 MLE thin film leads the progressive disappearance of the InPd diffraction spots till a sharp (1 × 1) pattern is recovered above 690 K. In the high coverage regime (from 4 to 35 MLE), the formation of three rotational domains of a *bcc*-In_7Pd_3 compound with (110) orientation is observed. This In-rich phase probably grows on top of interfacial InPd(110) domains and is metastable. It transforms into a pure InPd(110) near-surface intermetallic phase in a temperature range between 500 and 600 K depending on the initial coverage. At this stage, the surface alloy exhibits core-level chemical shifts and valence band (VB) spectra identical to those of the 1:1 InPd intermetallic compound and resembling Cu-like density of states. Annealing at higher temperatures yields to a decrease of the In concentration in the near-surface region to about 20 at.% and a (1 × 1) LEED pattern is recovered. © *2014 AIP Publishing LLC*. [http://dx.doi.org/10.1063/1.4892408]

I. INTRODUCTION

The catalytic properties of Pd nanoparticles on oxide supports have recently received much attention for hydrogen production in the methanol stream reforming (MSR) process ($CH_3OH + H_2O \rightarrow CO_2 + 3H_2$).[1–6] They are considered as potential alternatives to Cu/ZnO catalysts used today by industry, offering an improved thermal stability as well as an enhanced activity and selectivity for MSR.[3,7,8] The high selectivity and activity towards MSR of Pd/ZnO, Pd/Ga_2O_3, and Pd/In_2O_3 was attributed to the formation of intermetallic compounds by reduction of the powder catalyst under H_2 at high temperature,[9,10] linked to a shift towards higher binding energies of the Pd d-band upon alloying, making the density of states (DOS) of the alloy resembling that of Cu metal.[11] However recent studies have shown that the formation of intermetallic compounds is a necessary but not sufficient condition to gain high selectivity.[12,13]

Many studies have been devoted to the electronic and crystallographic structure of Pd-M (M = Zn, Ga, or In) intermetallic phases, which is a prerequisite to understand the chemical reactivity of these prospective catalysts at a microscopic level. Most of them deal with ZnPd intermetallics and a recent review can be found in Ref. 14. The catalytic properties of Pd nanoparticles supported on ZnO are ascribed to the formation of a stable ZnPd intermetallic phase with a 1:1 concentration ratio and a tetragonal structure.[15,16] Experimental studies of the Zn/Pd(111) system reported the formation of different surface alloys as a function of temperature and coverages, including a near stoichiometric ZnPd phase. The latter one is characterized by an apparent p(2 × 2) low-energy electron diffraction (LEED) pattern corresponding in fact to 3 rotational domains of a p(2 × 1) structure resembling a tetragonal ZnPd(111) surface with alternating rows of Pd and Zn atoms. This near-surface intermetallic phase (NSIP) exhibits the expected Cu-like DOS as well as a rumpling of the outermost surface layer induced by an outward shift of the Zn atoms and an inward shift of the Pd atoms (into the bulk),[16,17] associated with a high CO_2 selectivity. Upon annealing the film above 550 K, the Zn concentration in the near-surface region decreases rapidly although an almost stoichiometric monolayer surface alloy remains in the topmost layer. This change in sub-surface chemistry is associated with an inversion of the surface buckling (*i.e.,* Pd-up/Zn-down) and an increased DOS at the Fermi level together with a loss of CO_2 selectivity.[18] Similar trends have also been reported for the Ga/Pd(111) system.[19] These results show that rather subtle modifications of the

 © 2014 AIP Publishing LLC

This article is copyrighted as indicated in the article. Reuse of AIP content is subject to the terms at: http://scitation.aip.org/termsconditions. Downloaded to IP: 193.50.135.4 On: Mon, 20 Oct 2014 10:14:55

surface alloys can have dramatic effects on their catalytic properties.

In contrast to the Zn-Pd and Ga-Pd systems, surface alloys in the In-Pd system have received much less attention although In_yPd_x/In_2O_3 are also highly active and selective supported catalysts.[20] Earlier work by Fink *et al.*[21–23] reported compound formation upon In deposition on Pd(100) surface using perturbed $\gamma\gamma$-angular correlation spectroscopy. A more recent report by Rameshan *et al.*[24] found that room temperature deposition of a 4 monolayer equivalents (MLEs) of In on Pd foil followed by subsequent annealing to 453 K yields an almost stoichiometric InPd NSIP exhibiting a Cu-like DOS similar to the ZnPd counterparts. *In situ* X-ray photoelectron spectroscopy (XPS) under near-ambient pressure demonstrated an almost 100% CO_2 selectivity in a temperature range between 493 and 550 K. A change towards CO selectivity upon annealing above 600 K is explained by a decrease in the In sub-surface content. This behavior presents some similarities with the ZnPd system. However little is known about the structure of such near-surface intermetallic InPd phases.

In this work, we investigate the alloying tendency and the structure of In thin films grown on the Pd(111) surface using a combination of experimental methods (XPS, LEED, and STM). We show that different phases form depending on the initial In coverage and annealing temperatures, each possessing different chemical compositions and structural/electronic signatures.

The paper is organized as follows. We first provide experimental details in Sec. II. The results are presented in Sec. III, first for the low coverage regime, then for higher coverages. The main findings are summarized in Sec. IV and compared with the existing literature on related Pd-M (M = Zn, Ga, or In) systems. We also discuss our experimental results in the light of a joint theoretical study of InPd surface alloys using first-principle calculations.[25]

II. EXPERIMENT

A well-polished Pd(111) sample was placed under ultra-high vacuum (UHV) conditions with base pressures below 1×10^{-10} mbar. An atomically smooth surface free of sub-surface carbon contamination was achieved by cycles of Ar^+ sputtering at 1 keV, followed by annealing to 1173 K, then O_2 exposure ($P_{O_2} = 10^{-6}$ mbar, 15 mn, 873 K) and a final flash annealing to 1173 K. After multiple cycles, a sharp (1 × 1) LEED pattern was obtained and the absence of surface contamination was verified by XPS analysis. Indium was deposited *in situ* using an e-beam evaporator (EFM3, flux monitored) with the sample held at room temperature in the scanning tunneling microscopy (STM) stage. Thin film growth was investigated from submonolayer coverage up to 35 monolayer equivalent (MLE). Here an MLE is defined as the exposure required to complete one monolayer as observed by STM. The coverage as determined from STM images is found to increase linearly with exposure in the submonolayer regime. The films were annealed at different temperatures measured using a pyrometer with the emissivity set to 0.1. The temperature was also measured with a K-type thermocouple attached on the manipulator at some distance from the sample. There is a linear relationship between both measurements with an offset of approximately 150° (thermocouple reading is lower than pyrometer reading).

A polycrystalline InPd sample was also used in the study. An ingot was prepared by induction melting with a nominal composition of $In_{47}Pd_{53}$. Then the ingot was annealed in an evacuated quartz glass tube sealed under Ar atmosphere up to 1248 K, maintained at this temperature for 36 h and then cooled down to room temperature at a rate of 10 K/min. The crystallographic structure was checked by powder x-ray diffraction (XRD) (space group $Pm\bar{3}m$, CsCl type, $a = 3.23$ Å). The final composition as determined by energy dispersive x-ray analysis was $In_{47}Pd_{53}$, consistent with the existence domain of the InPd.[26] The surface of the polycrystalline sample was prepared under UHV conditions by sputtering and annealing cycles (Ar^+, 1 keV, 973 K). The surface composition measured by XPS was $In_{53}Pd_{47}$, *i.e.,* within the compositional range of the InPd compound.

III. RESULTS

A. Low coverage regime ($\theta \leq 2$ MLE)

1. Room temperature deposition

Figure 1 shows a sequence of STM images of the In film on Pd(111) with increasing coverage up to $\theta \sim 2$ MLE. Small islands of irregular shape are observed on terraces in the early stage of the growth with no preferential nucleation at step edges. With increasing coverage, the number of islands increases, with no obvious coalescence, until completion of the first layer. Then the second layer grows with a similar behavior. The islands exhibit a dendritic shape indicative of a diffusion limited growth process. A similar behavior has been

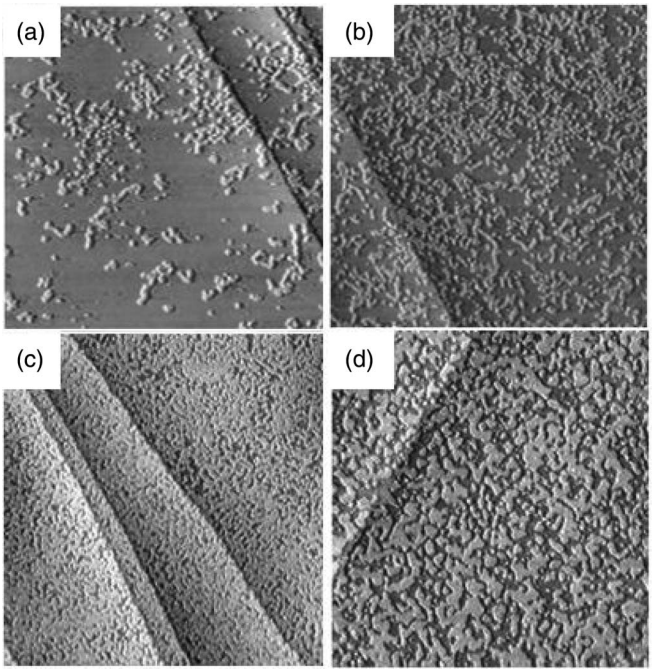

FIG. 1. STM images (200 × 200 nm^2) of the In thin film on Pd(111) surface for increasing coverage. (a) 0.2 MLE and (b) 0.4 MLE, $V = -2.0$ V, $I = 0.06$ nA; (c) 0.8 MLE, $V = +2.0$ V, $I = 0.06$ nA; (d) 1.7 MLE, $V = -1.4$ V, $I = 0.10$ nA.

This article is copyrighted as indicated in the article. Reuse of AIP content is subject to the terms at: http://scitation.aip.org/termsconditions. Downloaded to IP: 193.50.135.4 On: Mon, 20 Oct 2014 10:14:55

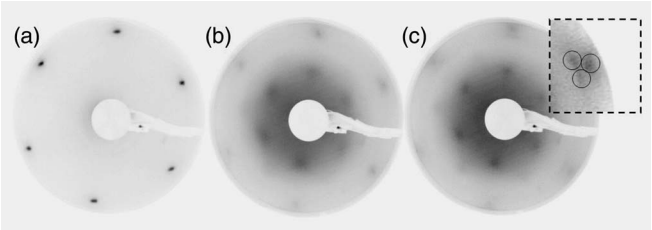

FIG. 2. LEED patterns of (a) the clean Pd(111) surface and after dosing (b) 1 MLE and (c) 2 MLE of In at room temperature. All patterns were recorded at an incident beam energy of 55 eV. The dotted rectangle in (c) is a blow-up of one of the outermost diffraction spots showing that they are actually poorly defined triplets.

observed in a study of Zn thin films on Pd(111).[27] The Pd step height is measured at 2.25 ± 0.05 Å corresponding to the theoretical Pd(111) interplanar spacing. The height of the islands is measured at 2.15 ± 0.05 Å.

Figure 2 shows the LEED patterns of the clean Pd(111) surface (Fig. 2(a)) and after dosing 1 MLE (Fig. 2(b)) and 2 MLE of In (Fig. 2(c)) at room temperature. Already at 1 MLE, a new pattern starts to appear which is slightly improved at 2 MLE coverage. The LEED patterns are quite diffuse in both cases and could be interpreted as either a (2 × 2) reconstruction or three rotational domains of a (2 × 1) reconstruction or three rotational domains of another structure resembling a (2 × 1) reconstruction. However, at 2 MLE, the outer spots appear to be poorly defined triplets (see blow-up in Fig. 2(c)), which rules out the first two hypothesis.

At this stage, the film is not sufficiently ordered to obtain atomically resolved STM images. However, domains can be identified exhibiting atomic rows, rotated by 120° from each other. The formation of these domains suggests that intermixing already occurs at room temperature. Further evidence for intermixing is provided by the core-level XPS data shown in Fig. 3. The Pd 3d core-level lines of the clean Pd(111) substrate can be fitted with a bulk and a surface contribution as described in Ref. 10. With increasing coverage, an additional peak grows on the high binding energy side, which is further enhanced at high take-off angle of the photoelectrons to increase the surface sensitivity. This peak corresponds to the surface alloy contribution. The position of this additional peak is shifted from the bulk Pd peak by +0.65 eV at 1 MLE and by +0.9 eV at 2 MLE. The shift is however smaller than the binding energy shift (+1.0 eV) observed for the InPd polycrystalline reference sample, suggesting that the surface alloy formed at room temperature is different from the stoichiometric compound in this coverage regime. Core-level peak fitting of the Pd 3d line indicates that the alloy contribution is more symmetric than the Pd bulk peak. The asymmetry of metal core-level line shapes results from intrinsic energy losses through electron-hole pairs excitations across the Fermi level and thus depends on the local density of states (DOS) at the Fermi level ($N(E_F)$).[28,29] Therefore the more symmetric line shape of the alloy component indicates a reduced $N(E_F)$ in the surface alloy compared to the substrate DOS. Another observation is the disappearance of the shake-up satellite at +5.9 eV from the Pd $3d_{3/2}$ upon alloying. The intensity of the shake-up satellite depends on the weight of unoccupied Pd 4d character and its position above E_F.[30] The disappearance

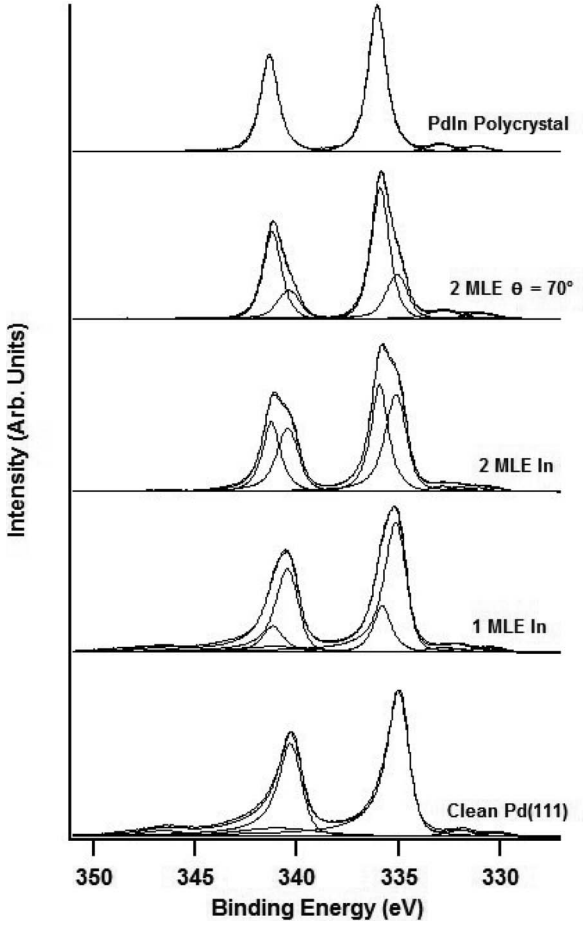

FIG. 3. XPS Pd 3d spectra of the clean Pd(111) surface, after dosing 1 and 2 MLE of In and of the clean polycrystalline InPd sample. All spectra were recorded at 45° take-off angle except for the second from the top spectrum which was collected at 70° to enhance surface sensitivity. A clear alloy component can be seen upon In dosing the Pd surface as well as the loss of the asymmetric tail and the disappearance of the shake-up satellites at 346.3 eV binding energy.

of the satellite upon alloying suggests that the Pd d band is being filled and shifted below the Fermi level upon alloying, a feature commonly observed upon intermetallic compound formation.[31] This is confirmed by XPS valence band measurements shown in Fig. 4. The main peak corresponds to the Pd d band which is shifted towards higher binding energies with increasing film thickness to resemble that of the polycrystalline reference sample. However at 2 MLE, the spectral weight within 2 eV below E_F is larger than for the polycrystalline sample. This is probably due to a Pd bulk contribution to the XPS signal in this low coverage regime. The chemical composition of the surface alloy formed at room temperature can be roughly estimated by considering the area of the In 3d peak and that of the alloy component of the Pd 3d peak, assuming that the In concentration is homogeneous across the alloy thickness. This gives a composition of $In_{47}Pd_{53}$ at 1 MLE and $In_{57}Pd_{43}$ at 2 MLE.

2. Annealing 1 MLE thin films

Upon successive annealing of the 1 MLE thin film up to 690 K, the broad diffraction spots observed at 300 K

This article is copyrighted as indicated in the article. Reuse of AIP content is subject to the terms at: http://scitation.aip.org/termsconditions. Downloaded to IP: 193.50.135.4 On: Mon, 20 Oct 2014 10:14:55

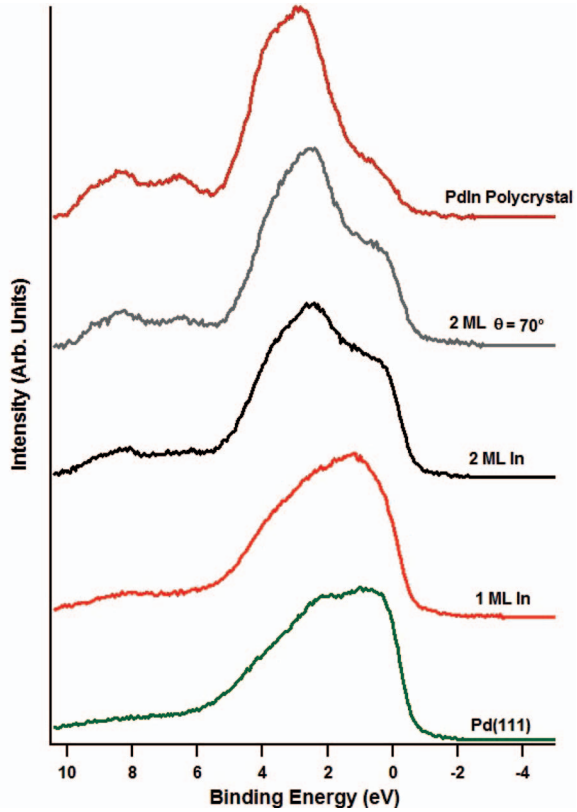

FIG. 4. Experimental XPS VB spectra of the clean Pd(111) surface, after dosing 1 and 2 MLE of In and of the clean polycrystalline InPd sample. All spectra were recorded at 45° take-off angle except for the second from the top spectrum which was collected at 70° to enhance surface sensitivity.

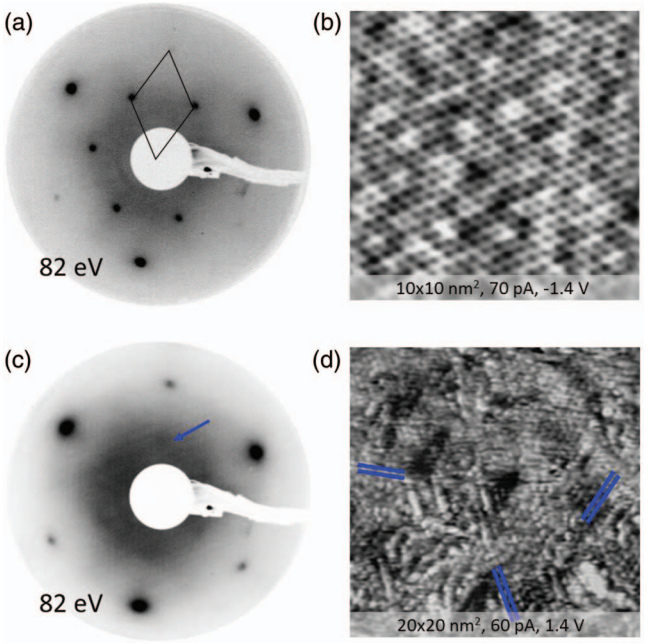

FIG. 5. (a) LEED pattern of the 1 MLE In film on Pd(111) after annealing at 690 K and (b) corresponding STM image (10×10 nm^2, V = −1.4 V, I = 0.07 nA). (c) LEED pattern of the 2 MLE In film on Pd(111) after annealing at 690 K and (d) corresponding STM image (20×20 nm^2, V = +1.4 V, I = 0.06 nA). Atomic rows can be distinguished according to three different orientations as indicated by straight lines in (d). The arrow in (c) points towards one of the diffuse spots arising from the surface alloy.

vanish and are replaced by a new well ordered $(\sqrt{3} \times \sqrt{3})$ R30° superstructure (Fig. 5(a)). The corresponding STM image is shown in Fig. 5(b). On large scale images, one observes a two phase mixture, one phase being disordered and covering less than 30% of the surface area, and an ordered phase with an hexagonal unit cell of dimension 4.75 Å consistent with the $(\sqrt{3} \times \sqrt{3})$ R30° superstructure observed by LEED. The STM contrast is not uniform, suggesting either chemical inhomogeneity and/or rumpling and/or structural imperfections. After annealing at 690 K, XPS core-level measurements show a decrease in the In content in the near-surface region. The estimated composition of the surface alloy is equal to $In_{41}Pd_{59}$. The uncertainty in this case is rather large because of the difficulty in extracting the Pd 3d alloy component out of the total Pd 3d line. The surface alloy is most likely confined in the topmost surface layers. Above 690 K, the LEED pattern evolves towards a (1x1) pattern. By XPS, the alloy component of the Pd 3d line has almost disappeared while the intensity of the In 3d line strongly decreases, indicating that the In atoms have either desorbed or diffused into the bulk.

3. Annealing 2 MLE thin films

Upon successive annealing of the 2 MLE thin film, the broad diffraction spots of the reconstruction observed at 300 K progressively vanish with no evidence of $(\sqrt{3} \times \sqrt{3})$ R30° ordering in this case. At 690 ±10 K, the LEED pattern shown in Fig. 5(c) is obtained where the (1×1) diffraction spots coexist with faint diffuse spots of the InPd surface alloy. An STM image of the corresponding film is shown in Fig. 5(d). The surface alloy is not well ordered but nevertheless domains can be seen presenting atomic rows. The chemical composition of the surface alloy is estimated at $In_{47}Pd_{53}$ following the peak fitting procedure described above. Further annealing of the 2 MLE film above 690 K leads to an even sharper (1×1) LEED pattern and a progressive loss of the In content in the near-surface region.

B. High coverage regime ($\theta \geq 4$ MLE)

After deposition of 4 MLE of In on Pd(111) at room temperature, the LEED pattern shown in Fig. 6(a) is observed. It is actually similar to the one obtained after 2 MLE deposition at room temperature except that the diffraction spots are now better resolved. The quality of the LEED pattern can be further improved by annealing the film up to 500 K as shown in Fig. 6(b). At this stage, the LEED pattern can be described as consisting of three rotational domains of a rectangular structure. The three domains and their relationship with the Pd(111) substrate are depicted in the LEED pattern in Fig. 6(b). The domains are rotated by 60° from each other. By calibrating the reciprocal space using the LEED pattern of the clean Pd(111) surface recorded under the same experimental conditions, it is deduced that the rectangular surface unit cells have dimensions $a = 3.28 \pm 0.1$ Å and $b = 4.64 \pm 0.1$ Å. These values are close to those of the rectangular unit cell of InPd(110) ($a = 3.25$ Å and $b = 4.6$ Å) and are thus consistent

This article is copyrighted as indicated in the article. Reuse of AIP content is subject to the terms at: http://scitation.aip.org/termsconditions. Downloaded to IP: 193.50.135.4 On: Mon, 20 Oct 2014 10:14:55

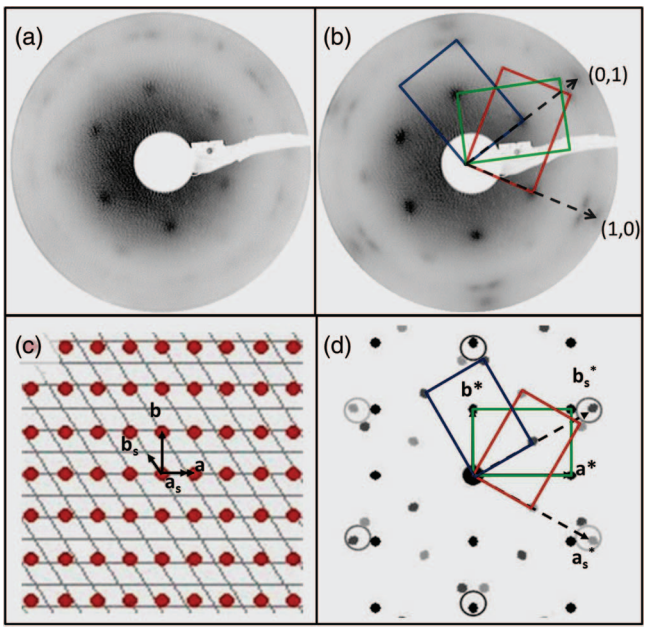

FIG. 6. LEED patterns of (a) the 4 MLE In thin film deposited on Pd(111) at room temperature and (b) after annealing at 500 K. The two patterns were recorded at an incident beam energy of 50 eV. The three rotational domains of the InPd(110) rectangular mesh are superimposed. The dashed arrows correspond to the Pd(111) lattice vectors. The first order substrate spots are in coincidence with the (0, 2) and (0, −2) spots of the InPd(110) domains. (c) Real space model of a single InPd(110) domain with lattice vectors (*a,b*) on a Pd(111) substrate with lattice vector (a_s, b_s). (d) Reciprocal space for three rotational domains of InPd(110) on Pd(111) substrate. Large circles indicate coincidence reciprocal lattice spots between the surface alloy and the substrate.

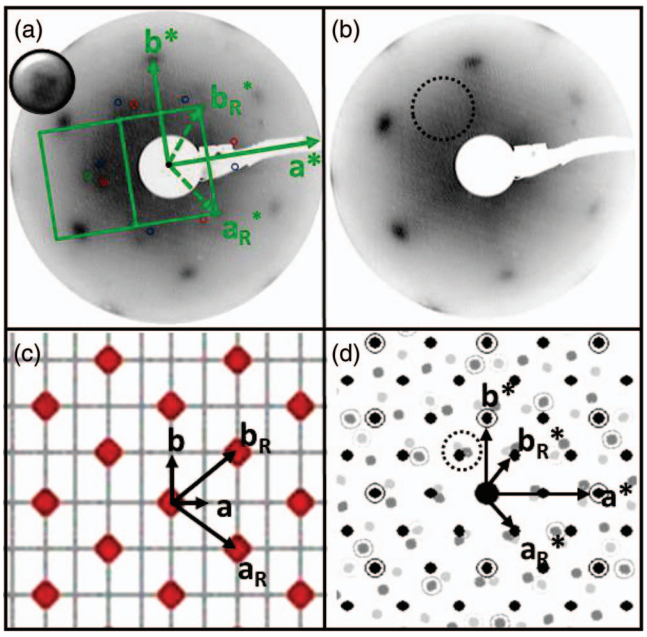

FIG. 7. (a) and (b) LEED patterns recorded at 21 eV beam energy for a 4 MLE In thin film on Pd(111) after annealing at 500 K and 550 K, respectively. The additional triplets of spots observed at 500 K disappear after annealing at 550 K. The reciprocal lattice vectors (a*, b*) of a single InPd(110) domain are outlined in (a) as well as those (a_R*, b_R*) of the larger structure. The equivalent centered rectangular net is also outlined for a single domain. The first nodes of the two other domains are outlined by empty circles in blue and red, respectively. The circular inset is a magnified view of one triplet of spots. The dotted circle in (b) indicates the position of the missing triplet after annealing at 550 K. (c) Real space model of the "c(4 × 2) reconstruction" with lattice vector (a_R, b_R) on a single domain of InPd(110). As explained in the text, the "c(4 × 2)" phase can alternatively be interpreted as In_7Pd_3-(110) domains. (d) Reciprocal space model for three rotational domains of c(4 × 2)-InPd(110) domains. The dotted circle indicates the triplet of spots observed in LEED patterns.

with the formation of three rotational domains of InPd(110) surface alloy on Pd(111). The orientation of the InPd(110) domains with respect to the Pd(111) substrate is determined by the coincidence of the (0,2) and (0,−2) reciprocal lattice spots of the InPd overlayer with the (0,1) and (0,−1) or (−1,0) and (1,0) or (−1,1) and (1,−1) substrate spots, respectively, hence the three rotational domains observed. A schematic of the model is shown in Figs. 6(c) and 6(d), in both real and reciprocal space. Considering the bulk parameters of Pd and InPd compounds, this locking into registry would imply a small lattice expansion of the surface alloy by 3.6%.

At low electron beam energy, additional triplet of spots appear for the same growth conditions; i.e., In deposition of 4 MLE at room temperature. They are slightly better defined after annealing up to 500 K (Fig. 7(a)) but disappear after annealing at 550 K (Fig. 7(b)). These triplets of spots do not originate from the InPd(110) domains themselves but correspond to a structure possessing a larger unit cell. The reciprocal lattice vectors (a_R*, b_R*) of this larger structure are shown in the LEED pattern in Fig. 7(a) together with the lattice vector (*a**, *b**) of a single InPd(110) domain. The larger structure corresponds to an oblique surface unit cell having parameters $a_R = b_R = 7.7 \pm 0.1$ Å and $\gamma = 71^\circ \pm 2^\circ$ or equivalently to a centred rectangular net with dimensions $a_R = 9.2 \pm 0.5$ Å and $b_R = 13 \pm 1$ Å. There are two possibilities to interpret this structure. From a purely geometrical point of view, it can be interpreted as a c(4 × 2) surface reconstruction of InPd(110) domains on the Pd(111) substrate as sketched in the model shown in Figs. 7(c) and 7(d) in both real and reciprocal space. However, the physical origin of such reconstruction is unclear. Considering the fact that its characteristic diffraction spots disappear upon further annealing at 550 K and that the In concentration in the near-surface region tends to decrease upon annealing as verified by XPS, we can suppose that this structural change is linked to a change in the chemistry of the diffracting overlayer. The In-Pd phase diagram contains several intermetallic compounds. On the In-rich side, one finds the In_7Pd_3 compound whose structure is closely related to the γ-brass structure type.[32] It has $Im\bar{3}m$ space group and a lattice parameter $a = 9.436$ Å. The surface unit cell in its (110) plane would thus have dimensions $a = 9.436$ Å and $b = 13.344$ Å, *i.e.,* close to the values (a_R, b_R) measured experimentally. Therefore this additional structure could alternatively be interpreted as three rotational domains of In_7Pd_3-(110) instead of c(4 × 2)-InPd(110) domains.

Atomically resolved STM images of the different structures are shown in Figure 8. The three rotational domains can be clearly observed in Fig. 8(a). The dimensions of the surface unit cell (Fig. 8(b)) are in agreement with the LEED measurements. Such structure is observed either directly after room temperature deposition of $\theta \geq 4$ MLE or after annealing up to 500 K to improve the structural quality. In these images,

This article is copyrighted as indicated in the article. Reuse of AIP content is subject to the terms at: http://scitation.aip.org/termsconditions. Downloaded to IP: 193.50.135.4 On: Mon, 20 Oct 2014 10:14:55

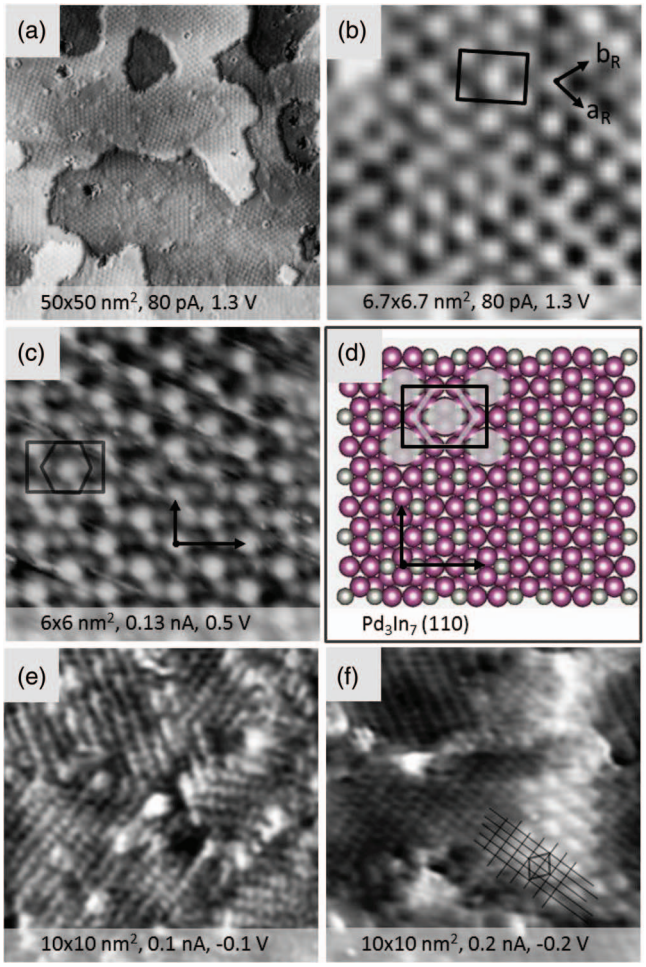

FIG. 8. (a) STM image of the 4 MLE In thin film on Pd(111) after annealing at 500 K showing multiple domains of the "c(4 × 2)" structure and (b) its atomic structure. The lattice vectors (a_R,b_R) are superimposed on the image, as well as the centered rectangular unit cell. (c) High-resolution STM image of the same structure obtained after room temperature deposition of 16 MLE In on Pd(111) showing additional contrast within the rectangular unit cell forming an elongated hexagon around each bright dots. (d) Structure model of the In_7Pd_3 (110) surface. (e) STM image of a 4 MLE In thin film on Pd(111) after annealing at 550 K showing multiple domains of InPd(110). (f) STM image of the same film as in (e) showing the coexistence of In_7Pd_3 (110) and InPd(110) phases and their orientation relationship.

one can only distinguished bright features at the nodes and at the center of the rectangular unit cell. Therefore it is not possible from such images to discriminate between the two structure models proposed earlier based on LEED patterns, *i.e.,* rotational domains of either In_7Pd_3(110) or c(4 × 2)-InPd(110). However, in rare cases, a better resolution could be achieved by STM as shown in Fig. 8(c) for a 16 MLE thin film after room temperature deposition. In addition to the bright dots at the nodes and centers of the rectangular mesh, one can distinguish 6 additional features surrounding each bright dot forming an elongated hexagon. The structure model of the (110) surface of the In_7Pd_3 intermetallic compound is shown in Fig. 8(d) assuming a bulk termination at dense puckered layer. At the nodes and center of the rectangular mesh, one finds a group of 4 atoms (2 Pd and 2 In atoms forming a cross) slightly protruding above the mean position of the plane. Each of these motifs is surrounded by 6 additional In atoms located at about 0.6 Å below. It is reasonable to assume that the groups of 4 protruding atoms are imaged as a bright dots by STM and that the 6 surrounding In atoms appear dimmer because they lie below the mean position of the surface plane. This model presents a good agreement with the experimental observations, supporting the formation of In_7Pd_3(110) domains rather than a c(4 × 2) reconstruction of InPd(110) domains. The film structure changes upon annealing at 550 K as can be seen in the STM image shown in Fig. 8(e). Now the film structure consists of three rotational domains of the InPd(110) phase in agreement with the LEED results. The dimensions of the surface unit cell measured by STM ($a = 3.25 \pm 0.1$ Å and $b = 4.6 \pm 0.1$ Å) are consistent with expected values. It is to be noted that the two structures, In_7Pd_3(110) domains and InPd(110) domains, are found to coexist at the surface, the former one being the dominant structure after room temperature deposition and annealing up to 500 K while the latter become the predominant structure after annealing to 550 K. The orientation relationship between the two structures is illustrated in the STM image shown Fig. 8(f), in which a In_7Pd_3(110) domain appears adjacent to a InPd(110) domain.

To summarize this section on In thin films ($\theta \geq 4$ MLE) on Pd(111), surface alloying is observed already after room temperature deposition leading to the formation of three rotational domains of a In_7Pd_3 compound with (110) orientation. This In-rich compound may grow directly on top of the Pd(111) substrate or may develop on top of InPd(110) domains formed as an interfacial layer in the early stage of the growth. Such near-surface layer is found to be stable up to annealing at 500 K but transforms into pure InPd(110) domains upon further annealing to 550 K. This sequence of surface phases has been observed for various coverages, including 4, 8, 16, and 35 MLE, the transition temperature always being in the range of 500 to 600 K. When the films are further annealed above 690 K, a LEED pattern similar to a Pd (1 × 1) pattern is recovered, consistent with what has been already observed for the 2 MLE thin film. Thus the InPd surface alloy is not stable in this temperature range and further In diffusion into the bulk or In desorption must take place. Figure 9 summarizes in a schematic way the different phases formed as a function of coverage and temperature.

Up to now, we have assumed the formation of In-Pd surface alloys based on structural information obtained by LEED and STM. The concentration in the near-surface region has been measured by XPS for the different coverages, before and after annealing in a temperature window of 500 to 600 K. The XPS core-level lines are shown in Figs. 10 and 11 for the different conditions. The composition of the near-surface alloy can be estimated assuming that the surface alloy is chemically homogeneous along the surface normal, a criterion which is most likely not satisfied. We nevertheless use this approximation in order to derive the basic trends in the chemical composition in the near-surface region. Before annealing, the surface alloy composition is In-rich and slowly evolves from $In_{64}Pd_{36}$ at 4 MLE to $In_{79}Pd_{21}$ at 35 MLE. After annealing, the In concentration in the surface alloy decreases to about 55%, *i.e.,* within the InPd compositional range, for all coverages above $\theta \geq 4$ MLE. A Pd bulk component in the Pd 3d

This article is copyrighted as indicated in the article. Reuse of AIP content is subject to the terms at: http://scitation.aip.org/termsconditions. Downloaded to IP: 193.50.135.4 On: Mon, 20 Oct 2014 10:14:55

<table>
<tr><td>> 690 K</td><td>(1x1)</td><td colspan="5" rowspan="2">(1x1)</td></tr>
<tr><td>690 K</td><td>(√3x√3)R30°</td></tr>
<tr><td>550-600 K</td><td colspan="2" rowspan="3">undefined</td><td colspan="4">3xInPd-(110)</td></tr>
<tr><td>500 K</td><td colspan="4" rowspan="2">3xIn$_3$Pd$_7$-(110)</td></tr>
<tr><td>300 K</td><td colspan="2">3xInPd(110)</td></tr>
<tr><td>T / θ</td><td>1 MLE</td><td>2 MLE</td><td>4 MLE</td><td>8 MLE</td><td>16 MLE</td><td>35 MLE</td></tr>
</table>

FIG. 9. Schematic summary of the different phases formed as a function of coverage and temperature.

line can still be observed directly after dosing up to 8 MLE, consistent with the probing depth by XPS. However, after annealing the 8 MLE, the Pd bulk component is not detected, which means that the thickness of the surface alloy has increased. The expected surface alloy thickness for a 1:1 stoichiometry at 8 MLE corresponds to 16 atomic planes equivalent to a thickness of 3.7 nm, i.e., larger than the XPS probing depth. Therefore annealing to 500–600 K is a necessary step to complete the alloy formation. Note that the chemical composition of the near-surface region measured after annealing the films at 500 K or 600 K is almost similar within the accuracy of the measurements, although this temperature window corresponds to the transition from the In-rich surface structure (In_7Pd_3) to the 1:1 InPd compound as determined by LEED and STM. However, for a given coverage, angle-dependent XPS measurements show a small increase of the In content for more surface sensitive conditions (20° take-off angle instead of 45°). These observations are consistent with a gradient of In concentration after room temperature deposition in this coverage regime, decreasing from surface to bulk and being more marked with increasing initial coverage. Probably the InPd compound is first formed at the interface region during growth and then the In_7Pd_3 phase is formed on top because the intermixing is not fast enough under these experimental conditions. Upon mild annealing, further diffusion takes place deeper in the bulk allowing the formation of a thicker InPd interface layer. In the temperature range 500–600 K, the In_7Pd_3 surface alloy should disappear to leave

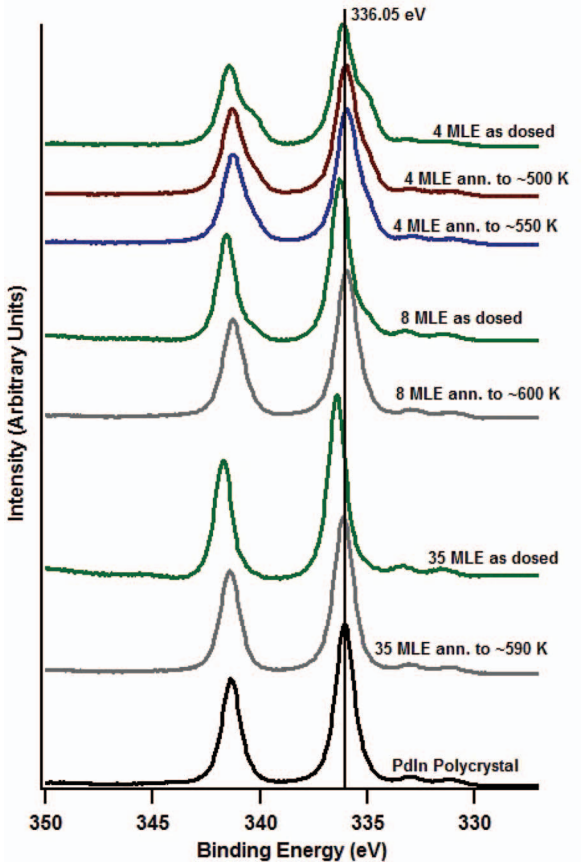

FIG. 10. XPS Pd 3d core-level lines for different film thicknesses, before and after annealing and for the reference InPd polycrystalline sample.

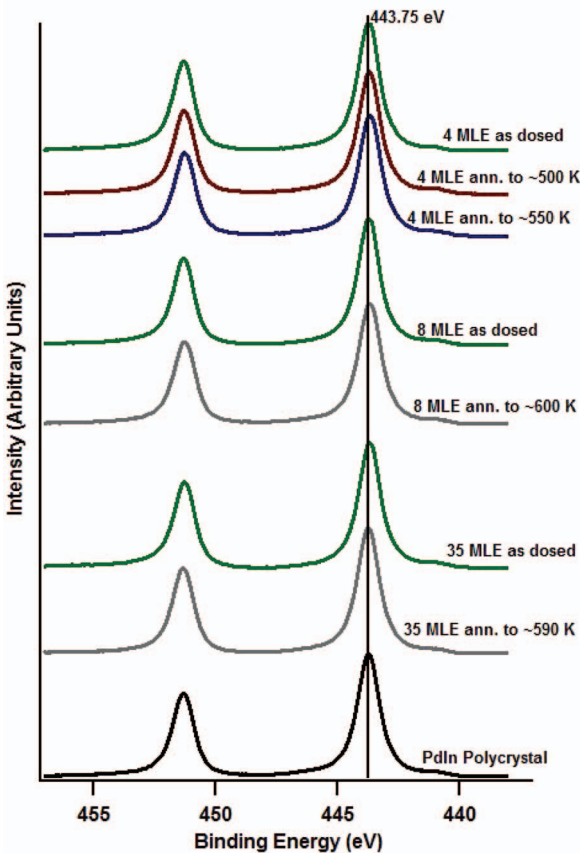

FIG. 11. XPS In 3d core-level lines for different film thicknesses, before and after annealing and for the reference InPd polycrystalline sample.

This article is copyrighted as indicated in the article. Reuse of AIP content is subject to the terms at: http://scitation.aip.org/termsconditions. Downloaded to IP: 193.50.135.4 On: Mon, 20 Oct 2014 10:14:55

TABLE I. Main characteristics of the XPS core-level spectra measured on the reference InPd polycrystalline sample.

	In $3d_{3/2}$	In $3d_{5/2}$	Pd $3d_{3/2}$	Pd $3d_{5/2}$
Position (eV)	451.30	443.77	341.35	336.05
FWHM (eV)	0.97	1.01	1.01	1.00

a single phase InPd surface alloy. This scenario is consistent with all presented observations. Note that due to the fact that such surface phase transformations are linked to diffusion and intermixing, the exact conditions under which a phase appears should not only depend on initial coverage and annealing temperature but also on the time elapsed between the deposition and the experimental observation.

As observed in Figs. 10 and 11, there is a systematic shift of the Pd 3d lines towards lower binding energy upon annealing the films while the In 3d line appears mostly at the same binding energy, independently of the conditions shown. We mention however the In $3d_{5/2}$ core-level line shifts to 443.5 eV for higher annealing temperature (690 K, not shown in Fig. 11), associated with a decrease of the In content. The final line shape and binding energies of Pd 3d and In 3d core-levels of the surface alloys after 500–600 K annealing are in good agreement with those measured for the polycrystalline reference samples (±0.05 eV). The main characteristics of the lines are provided in Table I. The XPS valence band spectra recorded for the same conditions are shown in Fig. 12. The

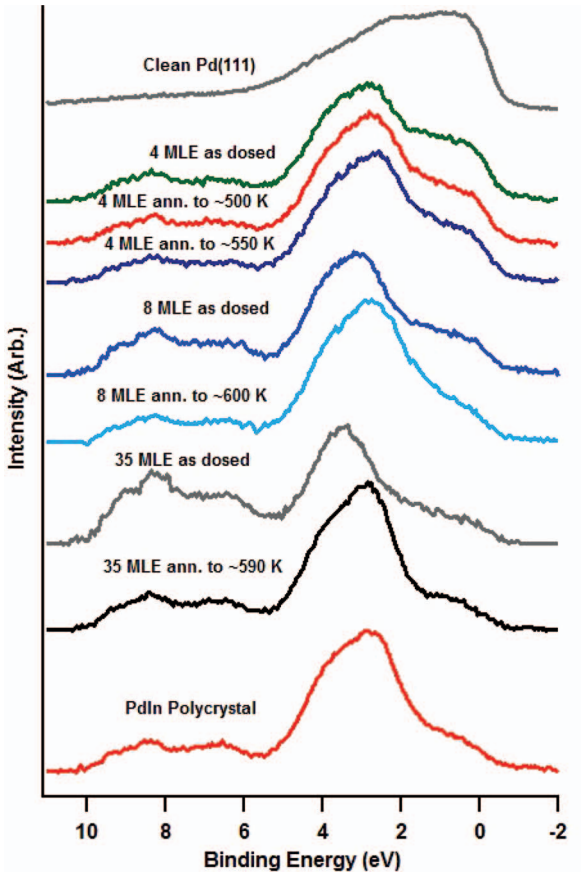

FIG. 12. XPS valence band data showed filling of Pd 4d bands to a Cu-like state upon dosing and annealing In/Pd(111) films.

broad main peak at approximately 2 to 4 eV below E_F arises from the Pd d band of the surface alloy and is being increasingly shifted to higher binding energies with increasing coverage after room temperature deposition. The spectral weight between 2 eV and E_F can be due to some Pd d states contribution of the InPd compound which has some sizable DOS in this energy range (see Ref. 25) as well as some additional contribution from d states of bulk Pd at low enough coverages. Upon annealing, the position of the main Pd d band shifts back to that measured in the reference polycrystalline sample. Simultaneously, the relative spectral weight within 2 eV below E_F decreases, consistent with an increase in the surface alloy thickness and thus a reduced Pd bulk contribution. The valence band spectra of the annealed films and of the polycrystal agree well and are resembling a "Cu-like" DOS expected for catalytic properties. However, the calculated DOS of the InPd compound shows significant difference with that of bulk Cu in the energy range of 1.5 eV to E_F, because of significant d states contribution in the intermetallic phase. This is similar to the cases of ZnPd and GaPd compounds.[33,34]

IV. DISCUSSION AND CONCLUSIONS

The experimental results indicate that surface alloying takes place at room temperature upon In dosing on the Pd(111) surface. This agrees with the theoretical prediction of a negative mixing enthalpy for the In_xPd_{1-x} solid solution in the dilute In limit reported in Ref. 25. In the low coverage regime ($\theta \leq 2$ MLE), the LEED patterns are consistent with the formation of three rotational domains of InPd(110) on top of the Pd(111) substrate. However, the structural quality of the surface alloy is rather low at this stage as evidenced by the diffuse diffraction spots. In addition, both the core-levels and valence band XPS spectra show that the surface alloy does fully exhibit the electronic structure characteristic of the stoichiometric phase under these conditions. Annealing the 1 MLE thin film up to 690 K yields a well ordered $(\sqrt{3} \times \sqrt{3})$ R30° superstructure with hexagonal unit cell dimension of 4.75 Å and an estimated surface alloy composition of $In_{41}Pd_{59}$. This observation is consistent with previous reports on a related system, Sn on Pd(111), for which a similar $(\sqrt{3} \times \sqrt{3})$ R30° phase was identified after annealing and ascribed to the formation of a Pd_2Sn monolayer surface alloy with *fcc* structure.[31,35,36] Calculations of segregation energies indicate that an In-doped layer buried in a Pd(111) substrate is preferentially located at the surface, therefore we expect this surface alloy to be confined in the outermost plane at this stage.[25] When the film is further annealed above 690 K, the In content in the near-surface region decreases and a (1×1) pattern is recovered in our case.

The $(\sqrt{3} \times \sqrt{3})$ R30° superstructure is not observed for thicker films. Successive annealing of the 2 MLE thin film leads the progressive disappearance of the InPd diffraction spots till a sharp (1×1) pattern is recovered above 690 K.

In the high coverage regime (from 4 to 35 MLE), LEED, STM, and XPS results indicate the formation of three rotational domains of a In_7Pd_3 compound with (110) orientation. This In-rich phase grows either directly on top of the Pd(111) substrate or on top of InPd(110) domains formed as an

This article is copyrighted as indicated in the article. Reuse of AIP content is subject to the terms at: http://scitation.aip.org/termsconditions. Downloaded to IP: 193.50.135.4 On: Mon, 20 Oct 2014 10:14:55

interfacial layer in the early stage of the growth. The near-surface layer is found to be stable upon annealing up to about 500 K and transforms into pure InPd(110) domains in a temperature range comprised between 500 and 600 K depending on the initial coverage. At this stage, the surface alloy exhibits core-level chemical shifts and VB spectra identical to those of the stoichiometric InPd intermetallic compound. In particular, a "Cu-like" DOS is observed. Annealing at higher temperatures leads to a decrease of the In concentration in the near-surface region suggesting that the surface alloy is not stable in this temperature range. A (1 × 1) LEED pattern is recovered at 690 K, together with a Pd-like DOS.

Our results are consistent with the conclusions of a previous XPS study on In-doped Pd foil performed by Rameshan *et al.*[24] In this work, a 4 MLE In thin film was deposited on a polycrystalline Pd substrate and the chemical composition of the NSIP as well as chemical shifts and VB were monitored as a function of the annealing temperature using synchrotron radiation based XPS. A high degree of alloying was also reported at room temperature. Upon successive annealing, the Pd 3d peaks gradually shifted towards lower binding energies associated with a decrease of the In content in the near-surface region and correlated with a transition from a "Cu-like" DOS to a more "Pd-like" (i.e., a shift of the d band center towards E_F). By varying the photon source energy (and hence the probing depth), a concentration gradient was highlighted from an In-rich next to the surface to a more In-depleted alloy in deeper layers. The concentration gradient was found to be more pronounced after low temperature annealing, from $In_{63}Pd_{37}$ at 0.4 nm inelastic mean-free path (IMFP) to $In_{51}Pd_{49}$ at 1 nm at 363 K annealing. These concentration values support our hypothesis that a In_7Pd_3 phase is formed on top of a 1:1 InPd interface layer. Annealing to 453 K yielded to a 1:1 In/Pd ratio in the near-surface region exhibiting a "Cu-like" DOS and In depth distribution similar to the MSR-selective multilayer ZnPd counterpart.[16] The 4 MLE In thin film annealed at 453 K was therefore used as a model surface to study the catalytic properties of the InPd system. In these experiments, the temperature was measured with a thermocouple directly attached to the sample, thus providing more reliable temperature values than those reported in the present work. Using the gradual shift of the Pd 3d peaks upon annealing as an internal temperature calibration, we determined that the 453 K-annealed state in Ref. 24 corresponds to our 500 to 550 K annealed state. In Rameshan *et al.*,[24] the structure of the 1:1 InPd NSIP was considered as that of a substitutional alloy with progressive replacement of Pd atoms by In within the Pd-*fcc* lattice with no relationship with bulk intermetallic phases of the In-Pd system. Our STM and LEED results show that the structure of the surface alloys formed on the Pd(111) substrate under similar conditions actually corresponds to intermetallic phases rather than substitutional alloys, either cubic CsCl-type InPd or *bcc*-In_7Pd_3 depending on the conditions. This conclusion is also consistent with a previous analysis by x-ray diffraction of In/Pd multilayer stackings on SiO_2 demonstrating the formation of these two compounds induced by room temperature interdiffusion.[37] The near-surface intermetallic phases are not stable upon annealing at higher temperatures. The In content decreases to reach a In/Pd ratio of about 20:80 and a (1 × 1) LEED pattern is recovered. This conclusion is again consistent with earlier reports indicating a similar In/Pd ratio throughout the near-surface region after annealing the 4 MLE thin film at 673 K.[24] Therefore the InPd surface alloys must be considered as metastable phases. This conclusion is consistent with the results of a theoretical study of InPd surface alloys using first-principles calculations demonstrating that In-doped Pd layers on Pd(111) are energetically more stable for In concentrations lower than 50 at.%.[25]

The formation of metastable phases with a global 1:1 composition is common to the related Zn/Pd(111)[10,16,18,27,38] and Ga/Pd(111)[19] systems. However, the composition changes are more gradual in the cases of Ga/Pd(111) and In/Pd(111) compared to Zn/Pd(111) for which a more pronounced plateau in the surface composition was observed between 400 and 550 K. For Zn/Pd(111), the 1:1 plateau correlates with the formation of an ordered (2 × 2) surface structure corresponding to 3 rotational domains of ZnPd(111)-(2 × 1)[27,39] whereas for Ga/Pd(111) the surface alloy is disordered in the same temperature range.[19] The onset temperatures for alloy formation were found to be different for Ga and Zn on Pd(111) (200 K for the former versus 300 K for the latter). This was interpreted as a consequence of the larger thermodynamic driving force for Ga-Pd compound formation compared to Zn-Pd based on the calculated cohesive energies. The onset alloying temperature was not determined in the present study but is lower or equal to 300 K. This is consistent with the cohesive energy calculated for the InPd compound (−3.57 eV/atom)[25] which is intermediate between that of PdGa (−3.9 eV/atom)[19,40] and ZnPd (−3.0 eV/atom).[41] Concerning the orientation of the surface alloys, we found that the cubic 1:1 InPd NSIP adopts a (110) orientation with respect to the Pd(111) substrate whereas the 1:1 tetragonal ZnPd NSIP adopts a (111) orientation. In both cases, it corresponds to stoichiometric layers consisting of alternating atomic rows of Pd and In (or Zn) metals. Only one type of atomic rows is observed in corresponding STM images. For Zn/Pd(111), this feature can be ascribed to an outward shift of the Zn atoms and an inward shift of the Pd atoms (into the bulk) with respect to the bulk-terminated geometry as demonstrated by DFT calculations.[39,41] This is consistent with the lower elemental surface energy of Zn compared to Pd. A similar effect is expected to occur on the InPd surface alloy, as the elemental surface energy of In is also much lower than that of Pd. Such type of surface relaxation can have a significant effect on the surface reactivity and is investigated theoretically in the part II of this article (Ref. 25).

ACKNOWLEDGMENTS

This work was supported by the ANR CAPRICE 2011-INTB 1001-01, the European C-MAC consortium and COST Action CM0904 "Intermetallic compounds as catalyst for steam reforming of methanol (IMC-SRM)."

[1]D. R. Palo, R. A. Dagle, and J. D. Holladay, Chem. Rev. **107**, 3992 (2007).
[2]N. Iwasa, S. Masuda, N. Ogawa, and N. Takezawa, Appl. Catal. A **125**, 145 (1995).

This article is copyrighted as indicated in the article. Reuse of AIP content is subject to the terms at: http://scitation.aip.org/termsconditions. Downloaded to IP: 193.50.135.4 On: Mon, 20 Oct 2014 10:14:55

[3]N. Iwasa and N. Takezawa, Top. Catal. **22**, 215 (2003).
[4]H. Gabasch, A. Knop-Gericke, R. Schlögl, S. Penner, B. Jenewein, K. Hayek, and B. Klötzer, J. Phys. Chem. B **110**, 11391 (2006).
[5]S. Liu, K. Takahashi, and M. Ayabe, Catal. Today **87**, 247 (2003).
[6]S. Liu, K. Takahashi, K. Uematsu, and M. Ayabe, Appl. Catal. A **277**, 265 (2004).
[7]D. L. Trimm and Z. I. Önsan, Catal. Rev. **43**, 31 (2001).
[8]N. Takezawa and N. Iwasa, Catal. Today **36**, 45 (1997).
[9]H. Lorenz, S. Turner, O. I. Lebedev, G. V. Tendeloo, B. Klötzer, C. Rameshan, K. Pfaller, and S. Penner, Appl. Catal. A **374**, 180 (2010).
[10]A. Bayer, K. Flechtner, R. Denecke, H. Steinruck, K. Neyman, and N. Rosch, Surf. Sci. **600**, 78 (2006).
[11]K. Nozawa, N. Endo, S. Kameoka, A. P. Tsai, and Y. Ishii, J. Phys. Soc. Jpn. **80**, 064801 (2011).
[12]M. Friedrich, D. Teschner, A. Knop-Gericke, and M. Armbrüster, J. Catal. **285**, 41 (2012).
[13]M. Friedrich, S. Penner, M. Heggen, and M. Armbrüster, Angew. Chem. Int. Ed. **52**, 4389 (2013).
[14]M. Armbrüster, M. Behrens, K. Fttinger, M. Friedrich, É. Gaudry, S. K. Matam, and H. R. Sharma, Catal. Rev. Sci. Eng. **55**, 289 (2013).
[15]S. Penner, B. Jenewein, H. Gabasch, B. Klötzer, D. Wang, A. Knop-Gericke, R. Schlögl, and K. Hayek, J. Catal. **241**, 14 (2006).
[16]C. Rameshan, C. Weilach, W. Stadlmayr, S. Penner, H. Lorenz, M. Havecker, R. Blume, T. Rocha, D. Teschner, A. Knop-Gericke, R. Schlögl, D. Zemlyanov, N. Memmel, G. Rupprechter, and B. Klötzer, J. Catal. **276**, 101 (2010).
[17]C. Rameshan, W. Stadlmayr, C. Weilach, S. Penner, H. Lorenz, M. Hävecker, R. Blume, T. Rocha, D. Teschner, A. Knop-Gericke, R. Schlögl, N. Memmel, D. Zemlyanov, G. Rupprechter, and B. Klötzer, Angew. Chem. Int. Ed. **49**, 3224 (2010).
[18]W. Stadlmayr, C. Rameshan, C. Weilach, H. Lorenz, M. Haevecker, R. Blume, T. Rocha, D. Teschner, A. Knop-Gericke, D. Zemlyanov, S. Penner, R. Schlögl, G. Rupprechter, B. Klötzer, and N. Memmel, J. Phys. Chem. C **114**, 10850 (2010).
[19]W. Stadlmayr, V. Huber, S. Penner, B. Klötzer, and N. Memmel, J. Phys. Chem. C **117**, 19558 (2013).
[20]N. Iwasa, T. Mayanagi, N. Ogawa, K. Sakata, and N. Takezawa, Catal. Lett. **54**, 119 (1998).
[21]R. Fink, B. U. Runge, K. Jacobs, G. Krausch, B. Luckscheiter, R. Platzer, U. Wöhrmann, and G. Schatz, Hyperfine Interact. **78**, 309 (1993).
[22]R. Fink, T. Koch, G. Krausch, J. Marien, A. Plewnia, B.-U. Runge, G. Schatz, A. Siber, and P. Ziemann, Phys. Rev. B **47**, 10048 (1993).
[23]R. Fink, B. U. Runge, K. Jacobs, G. Krausch, J. Lohmuller, B. Luckscheiter, U. Wohrmann, and G. Schatz, J. Phys. Condens. Matter **5**, 3837 (1993).
[24]C. Rameshan, H. Lorenz, L. Mayr, S. Penner, D. Zemlyanov, R. Arrigo, M. Haevecker, R. Blume, A. Knop-Gericke, R. Schlögl, and B. Klötzer, J. Catal. **295**, 186 (2012).
[25]É. Gaudry, G. M. McGuirk, J. Ledieu, and V. Fournée, J. Chem. Phys. **141**, 084703 (2014).
[26]H. Okamoto, J. Phase Equilib. **24**, 481 (2003).
[27]G. Weirum, M. Kratzer, H. P. Koch, A. Tamtoegl, J. Killmann, I. Bako, A. Winkler, S. Surnev, F. P. Netzer, and R. Schennach, J. Phys. Chem. C **113**, 9788 (2009).
[28]G. D. Mahan, Phys. Rev. **163**, 612 (1967).
[29]G. K. Wertheim and P. H. Citrin, *Photoemission in Solids I* (Springer-Verlag, 1978).
[30]F. U. Hillebrecht, J. C. Fuggle, P. A. Bennett, and Z. Zonierek, Phys. Rev. B **27**, 2179 (1983).
[31]A. Pancotti, A. de Siervo, M. Carazzolle, R. Landers, and G. Kleiman, J. Electron Spectrosc. Relat. Phenom. **156-158**, 307 (2007).
[32]H. Flandorfer, J. Alloys Compd. **336**, 176 (2002).
[33]S. A. Villaseca, D. Kandaskolov, É. Gaudry, and M. Armbrüster, Z. Anorg. Allg. Chem. **640**, 753 (2014).
[34]K. Kovnir, M. Armbrüster, D. Teschner, T. Venkov, F. Jentoft, A. Knop-Gericke, Y. Grin, and R. Schlögl, Sci. Technol. Adv. Mater. **8**, 420 (2007).
[35]A. F. Lee, C. J. Baddeley, M. S. Tikhov, and R. M. Lambert, Surf. Sci. **373**, 195 (1997).
[36]M. Carazzolle, G. Kleiman, R. Landers, A. Pancotti, A. de Siervo, and E. Soares, J. Mol. Catal. A: Chem. **281**, 9 (2008).
[37]A. Wronkowska, A. Wronkowski, A. Bukaluk, M. Trzciński, and K. Okulewicz, Appl. Surf. Sci. **253**, 3367 (2007).
[38]W. Stadlmayr, S. Penner, B. Klötzer, and N. Memmel, Surf. Sci. **603**, 251 (2009).
[39]H. Koch, I. Bako, and R. Schennach, Surf. Sci. **604**, 596 (2010).
[40]J. Prinz, R. Gaspari, C. A. Pignedoli, J. Vogt, P. Gille, M. Armbrüster, H. Brune, O. Gröning, and R. Widmer, Angew. Chem., Int. Ed. **51**, 9339 (2012).
[41]Z.-X. Chen, K. Neyman, A. Gordienko, and N. Rösch, Phys. Rev. B **68**, 075417 (2003).

This article is copyrighted as indicated in the article. Reuse of AIP content is subject to the terms at: http://scitation.aip.org/termsconditions. Downloaded to IP: 193.50.135.4 On: Mon, 20 Oct 2014 10:14:55